*Journal of Engineering Physics and Thermophysics, Vol. 82, No. 2, 2009*

# THEORETICAL AND EXPERIMENTAL STUDY OF THE PROCESSES OF WATER PURIFICATION IN A BIOFILTER

**I. G. Dueck**[a] **and S. V. Pyl'nik**[b]

UDC 628.353.153:519.67

*This paper presents the results of experimental measurements of substrate concentrations characterizing the efficiency of polluted water purification by a drop biofilter. A model describing the process of purification based on the diffusion-kinetic approach is presented. A good agreement between the experimental and theoretically calculated characteristics of the purification process has been shown. A simple semiempirical relation for estimating the operation of the drop biofilter is given.*

***Keywords:*** *biofilter, modeling, film erosion, approximate estimates, experiment.*

**Introduction.** Biopurification of water is carried out, e.g., by passing it through a charge of dispersed material with a high specific surface. The surface of particles is a habitat of microorganisms forming a biofilm [1, 2]. Impurities present in the water can serve as a nutrient substrate for microorganisms. Impurities are supplied to microorganisms in a convective-diffusion way from water to the biofilm surface and by a diffusion mechanism in the bulk of the biofilm where the microorganisms mineralize these impurities, and the gaseous products of enzymatic metabolic reactions are carried back into the water.

Biofilters are used successfully in cleaning water from various pollutants [3–10]. The stable effective operation of the biofilter is determined by a number of factors both promoting multiplication of microorganisms (conditions of the biochemical reaction, transport intensity of impurities and metabolic products) and inhibiting this process (film erosion by water flow, filling of charge pores, inhibition of bioreactions by products of their own vital activity).

Recent years have seen a rising interest in biofilters. This is due to the application of new materials for particles in the charge and small energy expenditures. The further development of the biopurification technology will be promoted by the elaboration of effective methods for simulating the processes in purifying plants. In the present paper, a model for calculating the biopurification in a continuous reactor supported by experiments on a laboratory facility is proposed. Below, instead of empirical assumptions about the exponential dependence of the decrease in the substrate concentration on the distance from the inlet to a reactor with parameters having no clear physical meaning and determined from experiments [10], this law is calculated directly with the use of the kinetics and mass transfer. The approach used was proposed in describing the processes proceeding in the biofilm [11–13].

**Experimental Facility.** Below we describe measurements of the efficiency of purification of an artificially prepared water representing a low-concentration meat broth (the total inlet content of carbon in the aqueous solution was varied from 5 to 58 mg/l). Experiments were performed on a drop biofilter representing a vertical pipe with a working section length equal to 268 cm. The diameter of the pipe was 15 cm. The charge grains represented Raschig rings of height 1.67 mm, inner diameter 1.23 cm, and outer diameter 1.47 cm. Water was supplied to the reactor through a sprinkler in the form of a downflow of drops equidistributed over the reactor cross-section, and the trickling filtrate was removed upon reaching the bottom hole. Microorganisms on the particle surface represented mixed cultures. Samples of water were taken at both the reactor inlet and outlet and also at two other points at a distance of 78 and 173 cm from the inlet.

The following indices were measured:

1. *Total organic carbon.* Hard balls of the biofilm carried out by the flow were filtered off from the samples, and the water was investigated for the total organic carbon with the use of a TOC-analyzer of the Groeger&Obst company (Germany).

[a]Erlangen-Nuremberg University, Erlangen, D-91052, Germany; email: Johann.Dueck@uvt.cbi.uni-erlangen.de; [b]Tomsk University, 36 Lenin Ave., Tomsk, 634050, Russia. Translated from Inzhenerno-Fizicheskii Zhurnal, Vol. 82, No. 2, pp. 273–282, March–April, 2009. Original article submitted July 17, 2007; revision submitted June 24, 2008.

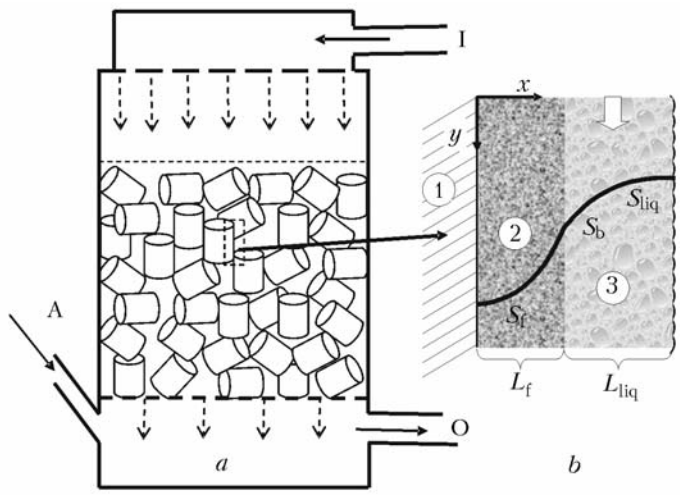


Fig. 1. Schematical representation of the water purification process: a) biofilter: I, inflowing water; O, outflowing water; A, air inflow; b) part near the ring surface: 1) ring; 2) biofilm of thickness $L_f$; 3) water film of thickness $L_{liq}$.

2. *Specific mass of the biofilm.* At the same sampling points as for the analysis of water, ten rings were taken out. The weight difference of rings covered with the biofilm and without it gives the mass of the biofilm. Knowing the surface of the rings and measuring the biofilm density, we determined its total volume. On the assumption of a uniform distribution of the biofilm over the surface of the rings its average thickness was calculated.

**Model of Water Purification in the Biofilter.** Water running down in the biofilter flows over the biofilm surface on particles (Fig. 1). The flow rate of water is selected so that it flows around the porous charge grains in the form of film and there is enough air between grains to provide aerobic microorganisms with oxygen.

1. Through the biofilm-water layer interface transport of the substrate into the biofilm occurs, so that in the direction of the flow ($y$) the substrate concentration in the water decreases:

$$Q_2 \frac{dS_{liq}(y)}{dy} = -\beta_w (S_{liq}(y) - S_b(y)), \tag{1}$$

where the value of the substrate concentration on the biofilm surface $S_b$ is not known in advance.

2. The distribution of the substrate concentration in the biofilm is described by the equation

$$D_f \frac{\partial^2 S_f}{\partial x^2} = q \frac{S_f}{K + S_f} X_f \tag{2}$$

with the boundary conditions

$$\frac{\partial S_f}{\partial x} = 0 \quad \text{at} \quad x = 0 \quad \text{and} \quad \beta_w (S_{liq} - S_f(L_f)) = D_f \frac{\partial S_f}{\partial x} \quad \text{at} \quad x = L_f; \quad S_{liq}(L_f(y)) = S_b(y). \tag{3}$$

The biomass production rate is equal to the death rate of microorganisms taken, as in [6–8], proportional to the squared concentration of the active biomass:

$$Yq \frac{S_f}{K + S_f} X_f = bX_f^2. \tag{4}$$

Equations (2) and (4) lead jointly to the relation

$$D_{\mathrm{f}}\frac{d^2S_{\mathrm{f}}}{dx^2}=\frac{q^2Y}{b}\left(\frac{S_{\mathrm{f}}}{K+S_{\mathrm{f}}}\right)^2. \tag{5}$$

3. The biofilm thickness is determined by the equality of the production rate of biomass across the whole width and the rate of its ablation:

$$\frac{Yq}{\rho}\int_0^{L_{\mathrm{f}}}\frac{S_{\mathrm{f}}}{K+S_{\mathrm{f}}}X_{\mathrm{f}}dx=rL_{\mathrm{f}}. \tag{6}$$

In view of (4)–(6) the biofilm thickness is defined as

$$L_{\mathrm{f}}=\frac{Y}{r\rho}\beta_{\mathrm{w}}(S_{\mathrm{liq}}-S_{\mathrm{b}}). \tag{7}$$

A major quantity found from the calculation is the quantity of substrate taken up from the water by the film. Finding the diffusion flow of the substrate into the film $J = D_{\mathrm{f}}\left.\frac{dS_{\mathrm{f}}}{dx}\right|_{z=L_{\mathrm{f}}}$ from Eq. (5) at the boundary conditions (3) and equating it to the substrate flow from the water into the film $J = \beta_{\mathrm{w}}[S_{\mathrm{liq}}(y) - S_{\mathrm{b}}]$, we obtain equations for finding $S_{\mathrm{b}}$.

Analysis of problem (3), (5) shows [14] that two reaction regimes can be distinguished: 1) in a relatively thick film, substrate consumption occurs not across its whole width, but only in the water-contacting layer (diffusion regime, unsaturated biofilm); 2) a relatively thin film is saturated with substrate due to the diffusion and its consumption occurs across its whole width at an approximately equal rate (kinetic regime, saturated biofilm). The expressions for the flow in both regimes have the form:

for unsaturated biofilm

$$J=\beta_{\mathrm{w}}[S_{\mathrm{liq}}(y)-S_{\mathrm{b}}]=\sqrt{\frac{KYq^2D_{\mathrm{f}}}{b}}\sqrt{2\left(1+\frac{S_{\mathrm{b}}(y)}{K}-\frac{1}{1+\frac{S_{\mathrm{b}}(y)}{K}}-2\ln\left(1+\frac{S_{\mathrm{b}}(y)}{K}\right)\right)}, \tag{8}$$

for saturated biofilm

$$J=\beta_{\mathrm{w}}[S_{\mathrm{liq}}(y)-S_{\mathrm{b}}]=\sqrt{\frac{KYq^2D_{\mathrm{f}}}{b}}\sqrt{\frac{3S_{\mathrm{b}}\left[1-\sqrt{rb\rho/(Yq)^2}\,\frac{S_{\mathrm{b}}(y)+1}{S_{\mathrm{b}}(y)}\right]}{1-\sqrt{rb\rho/(Yq)^2}}\frac{rb\rho}{(Yq)^2}}. \tag{9}$$

It has been shown in [14] that the regime of unsaturated biofilm at relatively small substrate concentrations ($S_{\mathrm{liq}} < K$) sets in at $r = 0.6r_{\mathrm{lim}}$.

The quantities $Q_2$, $\beta_{\mathrm{w}}$, and $r$ occurring in (1), (7) should be expressed in terms of the geometric characteristics of the column, individual rings, porosity of their packing, and the total water discharge $Q_\Sigma$.

The volume of the liquid running off the Raschig ring equals $Q_3 = 4\pi\tilde{R}Q_2$. Here $2\pi\tilde{R}$ is some average perimeter of the flow around the ring. For each individual ring the flow perimeter differs from the others depending on its random position in the charge. When the axis ring coincides with the reactor axis, then $2\pi\tilde{R} = 4\pi R$, and when the ring axis is perpendicular to the reactor axis, then $2\pi\tilde{R} = 2H$. To estimate $\tilde{R}$, let us use the mean between these two values: $\tilde{R} = R\left(1+\frac{H}{2\pi R}\right)$. Let us replace the volumetric rate of flow past each grain by the total discharge through the

charge. If the area of the column section is $R_{col}^2$, then for $N$ grains present in this section $N\tilde{R}^2 = R_{col}^2(1-\varepsilon)$ holds. On the other hand, since water flows only along grains, $NQ_3 = Q_\Sigma$; therefore, $Q_2 = \frac{Q_\Sigma}{4\pi\tilde{R}}\left(\frac{\tilde{R}}{R_{col}}\right)^2 \frac{1}{1-\varepsilon}$. Let us introduce the specific volume flow per unit area of the reactor cross-section $Q = \frac{Q_\Sigma}{\pi R_{col}^2}$.

With the help of the theory of [15] in [16] for the mass transfer coefficient the expression

$$\beta_w = 0.62 D_{liq}^{2/3}\left(\frac{\tilde{g}^2}{\nu\tilde{R}^3}\frac{\tilde{Q}R}{\nu(1-\varepsilon)}\right)^{1/9} \tag{10}$$

was obtained. Here $\tilde{g} = \frac{2}{\pi}g$ is the mean value for the free fall acceleration determined by the random orientation of the grain in the charge.

The measurements of the ablation coefficient of the biofilm in the investigated biofilter presented in [17] give a linear dependence of $r$ on the specific flow rate, which can be expressed by the formula

$$r = 2\cdot 10^{-4} Q\ . \tag{11}$$

Integrating (2) in view of (4), we arrive at the expression $YJ = b\int_0^{L_f} X_f^2 dz = b\langle X_f^2\rangle L_f$. Substituting in it $\langle X_f^2\rangle$ by $\langle X_f\rangle^2$, we get the estimate

$$\langle X_f\rangle = \sqrt{\frac{YJ}{bL_f}}\ . \tag{12}$$

Equations (1) and (8) or (9) permit determining the values of concentrations in the water and in the film along the reactor axis, and Eqs. (7) and (12) — the thickness and concentration of the active biomass.

**Approximate Solutions of the Equations of Water Purification in the Biofilter.** The specific features of the solution of the system of equations (1) (7), (8) or (9) are as follows. The mean concentration of the substrate in the biofilm $\langle S_f\rangle$ and, as a consequence, the mean concentration of the active biomass $\langle X_f\rangle$ are constant throughout the length of the working channel of the biofilter and depend at fixed diffusion-kinetic parameters on the erosion intensity. From (11) it follows that at fixed characteristics of the porous charge the erosion intensity depends only on the flow rate of the substrate solution. Consequently, $\langle S_f\rangle$ and $\langle X_f\rangle$ are related only to the flow rate of the liquid. This can easily be shown by factoring the mean value of the integrand in (6) outside the integral sign and combining (6) and (12):

$$\frac{(Yq)^2}{b\rho}\left\langle\frac{S_f}{K+S_f}\right\rangle = r\,, \tag{13}$$

$$\langle X_f\rangle = \frac{Yq}{b}\left\langle\frac{S_f}{K+S_f}\right\rangle\ . \tag{14}$$

Assuming in (13) $\left\langle\frac{S_f}{K+S_f}\right\rangle = \frac{\langle S_f\rangle}{K+\langle S_f\rangle}$ we get an explicit expression for the substrate concentration in the film

$$\frac{\langle S_f\rangle}{K} = \frac{\sqrt{\rho rb}}{Yq}\left(1-\frac{\sqrt{\rho rb}}{Yq}\right)^{-1}\ . \tag{15}$$

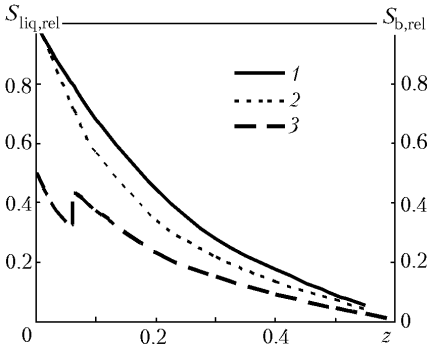


Fig. 2. Concentration profiles of the substrate down the stream of the liquid: 1) solution for $S_{liq}(y)$ with the use of (1), (10), and (11); 2) expression (18); 3) solution by (1), (10), and (11) for the concentration on the biofilm surface $S_b(y)$.

The highest possible value of $r$ in (13) is given by the limiting value for the erosion coefficient

$$r_{lim} = \frac{(Yq)^2}{b\rho} \left\langle \frac{S_{liq}(y)}{K + S_{liq}(y)} \right\rangle^2 . \tag{16}$$

At $r > r_{lim}$ the film is completely washed away by the flow.

If the erosion intensity at the biofilter inlet is sufficiently high but still lower than the limiting value, then for any chosen section the biofilm thickness is sufficiently small and the biofilm functions under conditions at which it will be saturated with the substrate across its whole width. In this case, Eq. (1) can be written in the form

$$Q_2 \frac{dS_{liq}(y)}{dy} = -\beta_w \left(S_{liq}(y) - \langle S_f \rangle\right) . \tag{17}$$

Unlike (1), expression (14) permits finding an analytical solution

$$\frac{S_{liq}(y) - \langle S_f \rangle}{S_{liq}(0) - \langle S_f \rangle} = \exp\left[-\frac{\beta_w}{Q_2} y\right]. \tag{18}$$

For calculations, the following diffusion kinetic parameters were taken: $D_{liq}$ = 0.8 cm$^2$/day, $D_f$ = 0.64 cm$^2$/day, $K$ = 0.01 mg/day, $q$ = 8 days$^{-1}$, $Y$ = 0.5, $b$ = 0.5 cm$^3$/(day/mg), $R_{col}$ = 7.5 cm, $R$ = 0.6775 cm, $H$ = 1.67 cm, $\varepsilon$ = 0.704.

Figure 2 presents, for $Q$ = 5.32 cm/min and the initial concentration $S_{liq}(0)$ = 0.00539 mg/cm$^3$, a comparison of the results of calculations of the decrease in the substrate concentration in water along the reactor channel obtained with the use of (17) and by the numerical solution of (1), (8), and (9). The results in Fig. 2 are given in coordinates $z = \frac{\beta_w}{Q_2} y$ (abscissa axis) and $S_{liq,rel} = \frac{S_{liq}(y) - \langle S_f \rangle}{S_{liq}(0) - \langle S_f \rangle}$ (ordinate axis). Here $\langle S_f \rangle$ is given by formula (15). The same figure shows also the change in the relative concentration of the substrate on the biofilm surface $S_{b,rel} = \frac{S_b(y) - \langle S_f \rangle}{S_{liq}(0) - \langle S_f \rangle}$ along $z$. At the inlet cross-section of the biofilter at the chosen initial value of the substrate concentration in the liquid the ratio $\frac{r}{r_{lim}(S_{liq}(y=0))}$ = 0.495.

In accordance with the initial condition, the curves for the numerical experiment and the calculation by (17) emanate from one and the same point $S_{liq}(0)$. Further, since the biofilm functions in the kinetic regime (the film is unsaturated), the approximate theoretical curve (17) derivates from the calculated curve.

TABLE 1. Measured Values of Substrate Concentrations $S_{liq}$ (mg/cm$^3$) for Various Flow Rates

| Variant number | $Q$, cm/min | $y$, cm | | | |
|---|---|---|---|---|---|
| | | 0 | 78 | 173 | 268 |
| 1 | 3.28 | 0.058 | 0.031 | 0.022 | 0.0172 |
| 2 | 4.47 | 0.026 | 0.016 | 0.012 | 0.0085 |
| 3 | 5.26 | 0.0055 | 0.0042 | 0.0038 | 0.0035 |
| 4 | 5.32 | 0.0096 | 0.0075 | 0.0059 | 0.0042 |
| 5 | 5.82 | 0.0086 | 0.0061 | 0.0049 | 0.0040 |
| 6 | 5.89 | 0.019 | 0.012 | 0.0084 | 0.0059 |
| 7 | 6.56 | 0.014 | 0.0091 | 0.0062 | 0.0058 |
| 8 | 10.63 | 0.0077 | 0.0062 | 0.0048 | 0.0047 |
| 9 | 11.32 | 0.011 | 0.0092 | 0.0072 | 0.0055 |

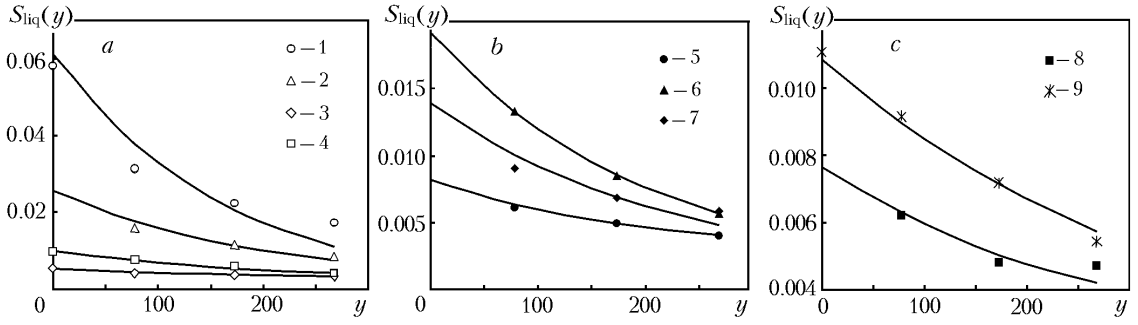


Fig. 3. Substrate concentration in the liquid $S_{liq}(y)$ versus the distance $y$ down the bioreactor column (curves show calculations, dots — experiments): a) relatively low flow rates of the substrate solution; b) moderate flow rate of the substrate; c) relatively high flow rates of the substrate solution. The curve number corresponds to the variant number in the table. $S_{liq}(y)$,

As the substrate concentration in the liquid flow decreases, the diffusion regime (the film is saturated) begins to dominate, and, as a result, the curves converge, as was predicted by the analysis. At the chosen coordinates the line corresponding to the $\langle S_f \rangle$ value coincides with the abscissa axis. It is seen that the substrate concentrations in the liquid flow $S_{liq}(y)$ and on the biofilm surface $S_b(y)$ tend to the $\langle S_f \rangle$ value as the substrate moves into the depth of the biofilter and the flow passes to the kinetic regime with saturated film.

The characteristic kink on the $S_b(y)$ curve points to the passing from the diffusion regime to the kinetic one. A more complete comparison between experimental and calculated data is possible with the help of numerical solutions.

**Comparison of Calculations and Measurements.** Calculations were performed on the basis of Eqs. (1), (8), (9) at the above parameters with varying rate of substrate flow through the reactor $Q$ and substrate concentration $S_{liq}(0)$ in water at the reactor inlet (column at $y$ = 0, see the table). Measurements were made at the $Q$ values given in the table.

The calculated value of $S_{liq}(0)$ for each variant was chosen from considerations of the maximum (in terms of the sum of squared deviations) closeness between the experimental points and the calculation curve. Such an approach is due to the fact that repeated measurements of the substrate concentration in water were hampered.

The change in $S_{liq}(y)$ along the working channel of the biofilter was measured.

Figure 3 presents the results of the calculations (curves) and the experimental values (dots) for all variants of the values of substrate flow rates given in the table. In all cases, there is a fairly good agreement between the experimental and calculated data.

Both the experiment and the numerical calculation show that for high flow rates $Q$ the efficiency of water purification, i.e., the ratio between the carbon concentrations at the reactor outlet and inlet, decreases. This is likely to be due to the reduction of the dwelling time of the substrate solution in the reactor in spite of some increase in the mass transfer intensity.

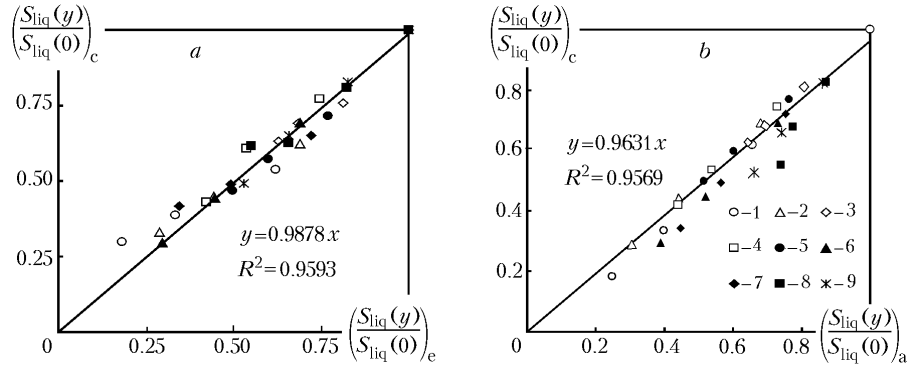


Fig. 4. Comparison between the substrate concentration $S_{liq}(y)$ calculated on the basis of the complete problem at all sampling points related to the $S_{liq}(0)$ value in the water layer (abscissa axis) and the same value obtained experimentally (a) and on the basis of the approximation dependence (20) (b). The curve number corresponds to the variant number in the table.

The approximate analytical solution (18) leads in most cases to considerable deviations from the measured values. The reason for this is the neglect of the internal diffusion resistance of the biofilm. The effective mass transfer coefficient calculated by the rule of addition of diffusion resistances can be estimated as

$$\beta = \beta_w \frac{D_f}{D_f + \beta_w L_f}. \tag{19}$$

In order not to complicate formula (18) it is desirable to take, in using (19), the $L_f$ value at the reactor inlet. On the basis of tests, we can propose an empirical formula with an effective mass transfer coefficient calculated as a geometric mean: $\beta_{a.g} = \sqrt{\beta(0)\beta_w}$, i.e., use instead of (18) the following expression:

$$\frac{S_{liq}(y) - \langle S_f \rangle}{S_{liq}(0) - \langle S_f \rangle} = \exp\left[-\frac{\beta_{a.g}}{Q_2} y\right], \tag{20}$$

where

$$\beta_{a.g} = \beta_w \left(1 + \frac{\beta_w L_f(0)}{D_f}\right)^{-\frac{1}{2}}. \tag{21}$$

The results of the comparison is shown in Fig. 4b and points to the fully justified application of formula (20).

The calculations provide an additional possibility of judging the behavior of other, not measured, variables defining the process of water purification such as the substrate flow into the biofilm and the biofilm thickness in each section of the biofilter. However, comparison between measured and calculated thicknesses of the biofilm (Fig. 5) does not always give a satisfactory result for several reasons, including the following ones:

1. Modeling of the biofilm as a smooth layer characterized by the thickness alone is obviously insufficient. Models describing two-dimensional films are rather complicated and are under development [18].

2. Measurements were taken after about a weak upon variation of the feed rate of the substrate solution or its concentration. During this time, probably, the microflora concentration and, accordingly, the substrate flow in the film manage to adjust themselves to the new conditions, and the corresponding change in the biofilm thickness strongly depends on the erosion intensity and requires much more time.

3. Measurements of the thickness of the biofilm through measurements of the mass or its volume may not be accurate enough, since they do not take into account the nonuniformity of the film distribution over the surface of grains.

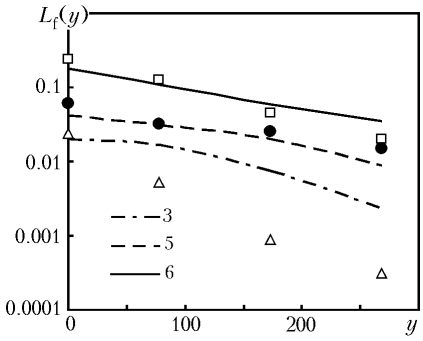


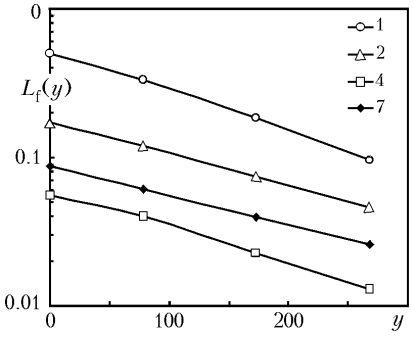


Fig. 5. Comparison of some of the calculated and measured thicknesses of the biofilm $L_f$ in various sections along the reactor $y$ and under various flow conditions: 3, 5, 6) variant number. $L_f$, $y$, cm.

Fig. 6. Calculated thickness of the biofilm $L_f$ versus the distance $y$ down the bioreactor column for low and moderate flow rates of the substrate solution: 1, 2, 4, 7) variant number. $y$, $L_f$, cm.

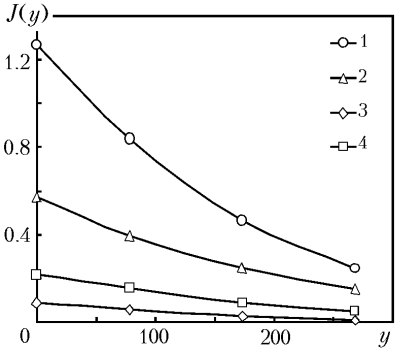


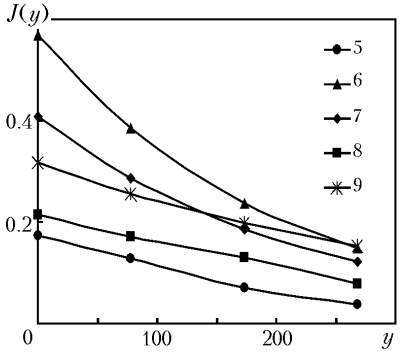


Fig. 7. Calculated substance flow into the biofilm $J$ versus the distance $y$ down the bioreactor column for relatively low flow rates of the substrate. The curve number corresponds to the variant number in the table. $J$, mg/(cm$^2$·day); $y$, cm.

It is important to know the film thickness, because this characteristic correlates with the substrate flow into the film. The calculated values of $L_f(y)$ and $J(y)$ for various $Q$ and $S_{liq}(0)$ from the table are given in Figs. 6 and 7.

Figure 6 shows the curves reflecting the change in the biofilm thickness along the working channel of the biofilter. It is seen that the biofilm thickness decreases with decreasing concentration of the substrate in the liquid flow, as is predicted by formula (7).

The decrease in $L_f$ with $y$ is due to the decrease in the substrate concentration in water. On the other hand, a decrease in $L_f$ leads to a decrease in the working volume of the biofilm, which in turn decreases the intensity of water purification.

Figure 7 presents the curves reflecting the change with $y$ in the substrate flow into the film. The substrate flow decreases with increasing $y$ for the above-mentioned reasons for all values of water flows in the reactor.

**Conclusions.** The developed theoretical model of water biopurification in the biofilter agrees well with the experimental data obtained on a laboratory biocolumn. The agreement between calculations and measurements of the decrease in the substrate concentration down the column is much better than the corresponding comparison for the film thickness. A simple semiempirical formula for calculating the process of water purification in a drop biofilter has been developed.

This work was supported by INTAS, grant 06-1000016-5798.

## NOTATION

$b$, death rate of microorganisms, $m^3/(kg \cdot sec)$; $D_f$, $D_{liq}$, diffusion coefficient in the biofilm and in the liquid, respectively, $m^2/sec$; $g$, $\tilde{g}$, free fall acceleration and its reduced value, respectively, $m/sec^2$; $J$, substrate flow into the biofilm, $mg/(cm^2 \cdot day)$; $H$, grain height in the charge (Raschig rings), m; $K$, Michaelis–Menten constant, $kg/m^3$; $L_f$, bio film thickness, m; $L_{liq}$, water film thickness, m; $N$, quantity of charge grains in the biofilter section; $Q_\Sigma$, flow rate of the substrate solution, $m^3/sec$; $Q_2$, flow rate of the substrate solution per width unit of the water layer, $m^2/sec$; $Q_3$, volume of liquid running off one grain every second, $m^3/sec$; $q$, maximum rate of the biochemical reaction, $1/sec$; $R$, $\tilde{R}$, radius of the charge grain and its average size, respectively, m; $R_{col}$, radius of the biofilter column; $r$, erosion coefficient, $1/sec$; $S$, substrate concentration, $mg/cm^3$; $S_b$, substrate concentration at the biofilm boundary, $mg/cm^3$; $S_f$, substrate concentration in the biofilm, $mg/cm^3$; $S_{liq}$, substrate concentration in the water, $mg/cm^3$; $X_f$, active biomass concentration; $Y$, yield factor of the biomass per mass unit of consumed substrate; $x$, coordinate across the biofilm channel, m; $y$, coordinate along the working channel of the biofilter, m; $z$, dimensionless coordinate along the working channel of the biofilter; $\beta$, effective mass transfer coefficient from the water layer to the biofilm, $m/sec$; $\beta_w$, mass transfer coefficient through the biofilm, $m/sec$; $\varepsilon$, porosity of the charge material in the biofilter; $\nu$, viscosity, $m^2/sec$; $\rho$, density of the biofilm material, $kg/m^3$. Subscripts: a, approximate; a.g, geometric mean; b, boundary; col, column; c, calculated; e, experimental; f, film; lim, limiting; liq, water; rel, relative.

## REFERENCES


1. T. A. Trifonova, N. V. Selivanova, and N. V. Mishchenko, *Applied Ecology* [in Russian], Akad. Pr. Traditsiya, Moscow (2005).
2. B. E. Rittmann B. E. and Perry L. McCarty, *Environmental Biotechnology: Principles and Applications*, McGraw-Hill, Boston (2000).
3. H. D. Janke, *Umweltbiotechnik*, Verlag Eugen Ulmer, Stuttgart (2002).
4. Tzu-Yang Hsien and Yen-Hui Lin, Biodegradation of phenol wastewater in a fixed biofilm reactor, *Biochem. Eng. J.*, **27**, 95–105 (2005).
5. A. Joss, E. Keller, A. C. Alder, T. Ternes, and C. S. McArdell, Removal of pharmaceuticals and fragrances in biological wastewater treatment, *Water Res.*, **39**, 3139–3152 (2005).
6. C. Cortes-Lorenzo, M. L. Molina-Munoz, B. Comez-Villalbat, R. Vilhez, A. Ramost, B. Rodelas, E. Hontoria, and J. Gonzales-Lopez, Analysis of community composition of biofilms in a submerged filter system for the removal of ammonia and phenol from industrial wastewater, *Biochem. Soc. Trans.*, **34**, 165–168 (2006).
7. J. Chung and B. E. Rittmann, Bio-reductive dechlorination of 1,1,1-trichloroethane and chloroform using a hydrogen-based membrane biofilm reactor, *Biotechnol./Bioeng.*, **97**, 52–60 (2007).
8. Xu Yan-bin, Xiao Hua-hua, and Sun Shui-yi, Study on anaerobic treatment of wastewater containing hexavalent chromium, *J. Zhejiang University SCIENCE*, No. 6, 574–579 (2005).
9. A. F. Ramos, M. A. Gomes, E. Hontoria, and J. Gonzales-Lopez, Biological nitrogen and phenol removal from saline industrial wastewater by submerged fixed-film reactor, *J. Hazard. Mater.*, **142**, Issues 1–2, 175–183 (2007).
10. G. Tchbanoglous, F. L. Burton, and H. D. Stensel, *Wastewater Engineering: Treatment, Disposal and Reuse*, 4th ed., McGraw-Hill, Inc., Boston (2003).
11. J. G. Dueck, S. Pylnik, and L. Minkov, Mathematical modelling of biofilm dynamics, *Proc. Eur. Symp. on Environ. Biotechnology*, ESEB 2004, Balkema Publishers (2004), pp. 545–547.
12. J. G. Dueck, S. V. Pylnik, and L. L. Min'kov, Modeling of the evolution of a water-purifying biofilm with allowance for its erosion, *Biophysics*, **50**, No. 2, 505–514 (2005).
13. S. Pylnik and J. Dueck, Calculation method of the water purification process in a biofilter, *Ecology of River's Basins*, ERB-2005, 2nd Int. Sci. Conf. 27.09–01.10 2005, Vladimir (2005), pp. 475–479.
14. J. G. Dueck, S. V. Pylnik, and L. L. Min'kov, On equilibrium thickness of a biofilm, *Teor. Osnovy Khim. Tekhnol.*, **41**, No. 4, 455–460 (2007).

15. V. E. Nakoryakov and A. V. Gorin, *Heat- and Mass Transfer in Two-Phase Systems* [in Russian], Inst. Teplofiz. SO RAN, Novosibirsk (1994).
16. J. G. Dueck, A. V. Gorin, E. Ferdinandova, and S. V. Pylnik, Experimental investigation of the mass transfer in a film biofilter, in: *Proc. Conf.* "*Fundamental and Applied Problems of Contemporary Mechanics*," Izd. Tomsk Univ., Tomsk (2006), pp. 497–499.
17. S. V. Pylnik, J. G. Dueck, and L. L. Min'kov, Experimental investigation of biofilm erosion, in: *Proc. Conf.* "*Fundamental and Applied Problems of Contemporary Mechanics*," Izd. Tomsk Univ., Tomsk (2004), pp. 138–139.
18. M. C. M. Van Loosdrecht, J. J. Heijnen, H. Eberl, J. Kreft, and C. Picioreanu, Mathematical modelling of biofilm structures, *Antonie van Leeuwenhoek*, **81**, Nos. 1–4 (2002), December, 245–256.